

DOI: 10.1002/ ((please add manuscript number))

Article type: Full Paper

Structure – Thermodynamic-property Relationships in Cyanovinyl-based Microporous Polymer Networks for the Future Design of Advanced Carbon Capture Materials

Ali Yassin, Matthias Trunk, Frank Czerny, Pierre Fayon, Abbie Trewin, Johannes Schmidt, and Arne Thomas**

Dr. A. Yassin, M. Trunk, F. Czerny, Dr. J. Schmidt, Prof. Dr. A. Thomas

Department of Chemistry, Division of Functional Materials, Technische Universität Berlin, Hardenbergstr. 40, 10623 Berlin, Germany

E-mail: aliyassin_lb@hotmail.com, arne.thomas@tu-berlin.de

Dr. P. Fayon, Prof. Dr. A. Trewin,

Department of Chemistry, Lancaster University, Lancaster, UK

Nitrogen-rich absorbents have been immensely tested for the capture of carbon dioxide yet until this date, the molecular engineering and design rules for solid absorbent materials do not show to be well grounded. We report here a family of *cyanovinylene*-based microporous polymers synthesized under metal-catalyzed conditions as promising candidates for advanced carbon capture materials. Of paramount importance is the discovery of a structure – property relationship where CO₂ sorption enthalpies have shown to be directly proportional to the weight% of incorporated functional group in these networks. Motivated by this finding, polymers produced under base-catalyzed conditions with tailored quantities of cyanovinyl content have shown a systematical tuning of the isosteric heats of adsorption to target values. Enthalpies of 40 kJ mol⁻¹ and amongst highest reported to date, in carbonaceous networks undergoing physisorption, were obtained as such. A six-point-plot reveals that this structure – thermodynamic-property relationship is linearly proportional, and could thus be perfectly fitted to tailor-made values prior to experimental measurements. Dynamic simulations show that the binding site forms a bowl shaped region within which the CO₂ is able to sit and interact with its conjugated surrounding, while theoretical calculations confirmed the increase

of available high energy CO₂ binding sites with the concentration of CN and associated C=C functionality in a network. We think our concept presents a distinct method for the future design of advanced carbon capture materials urgently needed on a global scale.

1. Introduction

As concluded from the recent scenarios developed by British Petroleum BP and the International Energy Agency, fossil fuel demands will continue to grow in the near future.^[1] This is further driven by the discovery of new and emerging unconventional sources, such as tight oil and shale gas, which are becoming more technically accessible.^[2] Meanwhile, continued CO₂ emissions have been associated with rising sea levels, ocean acidification, increased droughts, reductions in crop productivity and deaths due to infectious diseases.^[3] Still, it is predicted in addressing the problem of global climate change, that a cigarette-like addiction for fossil fuel usage may generate a long period of time in which people express sincere desire to convert to clean energy resources but accomplish little to achieve it.^[4] Until a zero carbon footprint could be reached, it seems of urgent priority now to bring forward new materials that would serve under the technical processes developed for CO₂ capture.

One such process is the post-combustion capture from flue gas, a predominantly CO₂/N₂ gas separation at relatively low pressures, which has been the most explored strategy to date since it could be readily retrofitted to existing power plants.^[5] However due to stability and selectivity concerns in addition to the large amounts of energy required for their regeneration, through different swing adsorption techniques, even the best carbon-capture materials nowadays are unfeasible for large-scale deployment.^[6] Originally, contributions in the field were meant to overcome the sequestration energy penalty of wet scrubbing methods, involving alkanolamines, and lead to the introduction of solid adsorbents, in particular porous ones, as potential solution to the problem. Zeolites, silica, activated carbons and metal-organic frameworks had become under intensive consideration^[7] while microporous polymer networks (MPNs) were much recently introduced as well.

MPNs attracted much attention due to their unique feature of combining high accessible surface areas with a wide range of functional groups while preserving chemical robustness and thermal stability, albeit in exchange of superior crystallinity.^[8] Cooper's group undertook sincere effort in investigating different MPNs for CO₂ capture and studied the effects of surface area,^[9] water co-adsorption^[10] and chemical functionality^[11] in several conjugated networks (CMPs). Zhou presented breakthrough uptakes of CO₂ by post-functionalizing PPN-6 based materials with polyamines and sulfonates.^[12] Yavuz also showed much attention for carbon capture and introduced different novel MPNs with attractive properties.^[13]

More Literature from 2016?

While considerable work is being conducted to investigate more advanced polymers for such applications, recognized by the escalation of reports in literature,^[14] the engineering rules for their molecular design seem without solid bases. It has been stated that tuning the thermodynamics of interaction between CO₂ and the adsorbent is one of the most crucial considerations in improving the energy efficiency of CO₂ capture.^[15] Isothermic heats of adsorption were certainly modified, for example by changing the nature of incorporated functional group,^[11,16] but the term "fine tuning" has been mistakenly, or probably too-optimistically, used in literature only to describe diverse experimental values and qualitative changes in heats of adsorptions. To the best of our knowledge indisputable tuning of enthalpy to precise tailor-made quantities was heretofore out of reach.

2. Experimental results and discussion

Here, we describe the synthesis, characterization and experimental gas sorption properties of a series of engineered MPNs produced under both metal-catalyzed and metal-free reaction conditions and demonstrate a prime example in which CO₂ enthalpies can be well tailored to definite values via manipulating the corresponding content of cyanovinylene bridges. Theoretical models of the amorphous polymers were generated and their structures and porosities were assessed, while binding sites of carbon dioxide in these networks and their

diffusion in the different cyanovinyl-based polymers were sampled by performing molecular dynamics simulations.

Although nitrogen-rich materials were immensely tested due to their high selectivities, still, the cyanovinyl linkage has not yet been investigated for carbon capture. Beyond such reason, our interest stems from the fact that this moiety could be generated via a green synthetic route through simple condensation reactions, in which water is the sole by-product.^[17]

2.1. Networks P1-P4 based on (benzene-1,3,5-triyl)tris(2-phenylacrylonitrile)

2.1.1. Synthesis of the metal-catalyzed polymers under optimized conditions for efficient coupling

Since at first we wanted to investigate metal-catalyzed polymer networks, the tris-iodinated derivative of (benzene-1,3,5-triyl)tris(2-phenylacrylonitrile), monomer 1 (Figure 1), was prepared in near-quantitative yields from commercially available compounds (Supporting Information, S1). Obtained single crystals reveal through X-ray diffraction that phenyl rings adopt a trans confirmation relative to one another in a monoclinic crystal system (Figure 1b, S11 and crystallographic data). The monomer was later used as tecton to generate three different metal-catalysed MPNs under optimized conditions; by coupling with tetrakis(4-ethynylphenyl)methane or 1,3,5-triethynylbenzene in a Sonogashira-Hagihara reaction, with Pd, to produce P2 and P3 respectively and by direct polymerization via Yamamoto coupling,^[18] with Ni, to produce P4 (Figure 1a and S1). As follows, the obtained networks have different weight percentages (wt%) of cyanovinylene content (precised in S2). CMP-1 termed here P1, was prepared as un-functionalized reference polymer free of cyanovinylene bridges. Under optimized synthetic conditions recently developed by our group,^[19] triple bonds in P1 are completely coupled excluding any homo-polymerization like seen in previous reports.^[20]

The obtained polymers, amorphous as concluded from powder XRD analysis (S3), were initially characterized with solid-state ¹³C NMR confirming the three corresponding

cyanovinyl chemical shifts at 108, 114 and 132 ppm in the functionalized polymers; P2, P3 and P4 (Figure 1c, S4). Further investigations by FT-IR spectroscopy also showed the *characteristic* $-CN$ stretching at $\sim 2220\text{ cm}^{-1}$ (S5). In both techniques these signals were absent for P1 as eventually expected.

2.1.2. Nitrogen Sorption properties of the MPNs **P1–P4** and their carbon uptake

The porosity of networks was analyzed by collecting nitrogen sorption isotherms on activated samples at 77 K revealing type I isotherms (Figure 2a) with BET surface areas exceeding $500\text{ m}^2\text{ g}^{-1}$ for P2 and P3. The largest quantities of N_2 uptake were observed at low relative-pressures indicative of adsorption into micro pores which is consistent with the pore size distribution calculated from their isotherms (S7). While CMP-1 is already known to be a very porous material, P1 consistently reaches a BET surface area of $1700\text{ m}^2\text{ g}^{-1}$ explaining its high carbon dioxide uptake at 273 K (Figure 2b). Measurements were also recorded at 298 K to calculate the isosteric heats of adsorption (Q_{st}) from dual-site Langmuir fits of the CO_2 isotherms. Likewise they were performed with N_2 to determine the networks' selectivities under flue-gas conditions (85:15 / $\text{N}_2:\text{CO}_2$) with single-gas isotherms (S8) using the ideal adsorbed solution theory (IAST) model.^[21]

Figure 2c depicts a table summarizing the gas sorption properties of the networks under different experimental conditions. P1, P2 and P3 show impressive CO_2 capture values exceeding 100 mg g^{-1} at 273 K and decreasing by around 40% at higher temperature. While this large uptake is attributed to the immense porosity in P1, it clearly relates to the cyanovinyl content in the other networks rendering it as very interesting building block for carbon capture. Even for P4 which shows small porosity,^[22] this functional group maintains the polymer with an uptake of 32 mg of CO_2 per 1 g of material. It is noted however that selectivities of these networks over N_2 were relatively poor. In analyzing the measured isosteric heats of adsorption we discovered a close-to-perfect linear correlation with reference to the corresponding percentages of functional group (Figure 2c framed values and S9). This

was inspired by similar well-studied relationships in π -conjugated systems which show strong dependence between structure and the corresponding electronic property for example.^[23] The relation obtained, $Q_{st} = 21.07 + 0.37(\text{wt}\%)$, predicts for instance, that a 45 wt% of incorporated functionality will result in a sorption enthalpy of 38 kJ mol⁻¹. This could be even tuned to values as high as 40 kJ mol⁻¹ if the weight content is increased to 50%.

2.2. Networks P5 and P6 based on (benzene-1,3,5-triyl)triacetonitrile

2.2.1. Synthesis of the base-catalyzed polymers under metal-free reaction conditions and their gas sorption properties

To further investigate this unprecedented structure – thermodynamic-property relationship we designed another set of MPNs under metal-free conditions this time, where monomer 2, (benzene-1,3,5-triyl)triacetonitrile (Supporting information S1) was condensed with commercially available terephthalaldehyde or benzene-1,3,5-tricarbaldehyde, in presence of a base, to produce P5 and P6 respectively. The only by-product of such polymerization is water (Figure 3a). The percentage of cyanovinylene bridges in these polymers are engineered to the definite values previously discussed, whilst solid state ¹³C NMR and FT-IR confirmed the corresponding structures (S3, S4).

Gas sorption measurements for P5 and P6 were collected under the same conditions of the previous networks (Figure 3b). Nitrogen isotherms show BET surface areas around 100 m² g⁻¹ (S7) which is expected in such relatively flexible systems, but captured CO₂ quantities still reach values of 90 mg g⁻¹. Indeed it has already been observed that BET surface areas do not directly dominate the carbon capture in polymer networks at low pressures.^[9] The uptake was accompanied by a huge 7 to 9 fold-increase of selectivities over nitrogen gas reaching values close to 100 for P6 (S10). Figure S9 shows the measured isosteric heats of adsorption from the CO₂ isotherms collected at 273 K and 298 K. The important contribution of the obtained data (Figure 3b framed values) confirms the discussed relation earlier. Indeed sorption enthalpies of P5 (with 44.7 wt% functional group) and P6 (with 50.5 wt%) show the predicted

values at ~ 38 and 40 kJ mol^{-1} respectively, as expected. P6 has one of the highest enthalpies reported to date in carbonaceous physisorbents for CO_2 ; the next upper values in literature being related to direct chemisorption.^[24] Plotting the enthalpy values of all the different networks (P1 to P6) as function of the cyanovinyl content reveals an excellent matching with the best-fitting line in Figure 3c. Noteworthy this relation holds true for polymers prepared under several reaction conditions that are entirely different, as illustrated earlier (S9).

2.2.2. Vacuum swing adsorption (VSA) and temperature-programmed desorption analysis (TPD) of the polymers P1–P6

The energy penalty suffered during the regeneration step of materials used for carbon capture is usually associated with their high affinity to CO_2 as the adsorption process is mostly of chemical nature and involves bond formations that are hard to break. We were able, through the presented concept, to generate networks with their highest enthalpy values tuned just below the chemisorption barrier ($45 - 55 \text{ kJ mol}^{-1}$) at which the regeneration is expected to require minimal energy. To test this, network P6 (40 kJ mol^{-1}) was cycled under conditions similar to vacuum swing adsorption (VSA) with an autosorb iQ2 automated analyzer. In every cycle the material was saturated with CO_2 up to 1 bar at room temperature. Desorption was followed by applying under-pressure, without any thermal heating, for an automated period of time during which the analyzer relaxes to some stable pressure. In average 4 minutes at 1 mbar and ambient temperature were enough for the complete desorption and regeneration of the material (Figure 4a, starting point of every isotherm). In addition, after 10 cycles there was not any apparent loss in uptake capacity, thus indicating the high stability and cyclability of this network (Figure 4a, end point of every isotherm).

To further investigate the physical nature of sorption in this network, temperature-programmed desorption analysis (TPD) was performed on saturated samples with CO_2 at 1 bar.^[25] Helium was used as carrier gas and the material was heated to elevated temperatures for the full evacuation of the host. TPD shows that carbon release starts slightly above 50°C

while most of the CO₂ is already desorbed before 80°C (Figure 4b). The enthalpy values of the networks, in addition to their straightforward regeneration under simple conditions, as demonstrated by the techniques, prove the physisorption character of CO₂ and contribute to their interest as being a cornerstone for designing new materials of higher surface areas with enhanced carbon uptakes whilst keeping this easy regeneration feature.

3. Dynamic simulations and the generation of network models

Generation of amorphous networks is challenging due to the lack of experimental data to aid the construction of a representative model. Furthermore the generation process is often limited to small cells that do not allow for modeling of the nano scale structure of the porous polymers which could have an influence on the final properties.

3.1. Construction of P1 – P6 network models

Here, we use an automated structure generation methodology for the cyanovinyl-based extended network materials that exploits GPU hardware for increased speed and size of simulation. This methodology is implemented in the *Ambuild* code that integrates with HOOMD-blue and DL_POLY molecular dynamic simulation codes.^{18-20??} For each polymer we seed an initial simulation cell with stoichiometric quantities of the respective building blocks and solvent molecules. We designate end group atoms and cap atoms, together with a number of structural and geometric rules that build the network in a chemically realistic manner (Figure 5, Structures C1 to D3).

For P1, we define the building blocks as 1,4,-diiodobenzene C1 and 1,3,5-triethynylbenzene D1 monomers with the cap atoms, respectively phenyl-I and ethynyl-H, being removed once a bond is formed between the respective phenyl-C and ethynyl-C end group atoms. Similarly, for P2 – P4 the common building block is defined as C2 (monomer 1), with the cap atom defined as the phenyl-I and the bonded phenyl-C as the end group. P2 is constructed from C2 and D2, P3 is constructed from C2 and D1, and P4 is constructed from C2 alone. For P5 and P6 the monomer units are not used as the chemistry is challenging to mimic the building

procedure, rather we define two further building units based on the resulting frameworks and monomer units; C3 based upon monomer 2, and D3 (1,3,5-triiodophenyl) based upon benzene-1,3,5-tricarbaldehyde. Thus, P5 is constructed from C3 and C1 and P6 is constructed from C3 and D3 (Table in Figure 5). In all cases bonding is tested between the respective cap atoms which are removed once a new bond is formed at the end groups based upon the geometrical and structural rules. For P5 and P6, any cap atom or functionality that remains at the end of the network's generation procedure is replaced with the respective terminal group expected for the synthetic procedure.

A number of molecular dynamic (MD) simulation loops are undertaken with structural sampling for potential bond formation. Upon bond formation, the structure undergoes a full, rigid-body geometry optimization before returning to the MD loops. The full building procedure is reported (Supporting Information, Section 12 and Table S2).

3.2. Structure and porosity assessment of the cyanovinyl-based MPN models

Here, we target network densities of $0.7 - 1.1 \text{ g cm}^{-3}$ as this range is commonly determined for similar CMP materials with similar porosity data. CMP materials with high surface areas tend to have low densities. The networks are generated in presence of solvent to get the target density then 'de-solvated' by removal of the solvent and further molecular dynamic and geometry optimization steps are undertaken to obtain the final network structures. P1 – P3 have densities between 0.76 and 0.81 g cm^{-3} obtained (SI, section 14), consistent with other CMP materials with similar surface area and porosity uptake properties where the experimental density has been determined.^{ref} P4 has a density of 0.76 g cm^{-3} , lower than expected given the relatively low surface area obtained experimentally. P5 and P6 have densities of 1.02 and 1.4 g cm^{-3} respectively, consistent with the low surface areas obtained experimentally. We believe that the increased density reflects the increased flexibility of the network formed and its ability to pack efficiently.

Comparison of elemental analysis of the generated network materials to the experimental data shows the same trend of the weight percentage of carbon decreasing and a weight percentage of nitrogen increasing going from P1 to P6 (SI, Table S3).

Geometric surface areas were calculated for each model and are shown in Supporting Information, Table S4. The trend in the calculated values is in broad agreement with that obtained experimentally with surface areas decreasing from P1 to P6. Calculated pore size distributions are shown in SI section 15. For P1 to P4 they range between 5 and 18 Å, broadly centered around 10-12 Å, in agreement with the ranges observed experimentally. P5 and P6 have pore sizes ranging between 5 and 10 Å, reflecting the increased density and efficient packing of the network. The experimental pore size distribution for all polymers shows the presence of mesopores with pore widths greater than 30 Å. It is not possible to take account of these larger pores as the unit cell size artificially restricts the pore width to the microporous region (SI, Figure S13).

3.3. Carbon dioxide binding sites in cyanovinyl-based MPNs Models

The binding energy of CO₂ to functional groups within the polymer network was assessed through density functional theory calculations with BSSE correction. A fragment of the P5 and P6 polymer was generated as a representative structure for the CN rich functionality of each polymer. The binding energy of the CO₂ molecule was calculated for a number of positions. A similar high energy binding site for P5 and P6 was found where the CO₂ is able to interact with a CN, C=C, and a phenyl ring with a binding energy of 23.35 and 21.13 kJ mol⁻¹ respectively. Interestingly, the binding site forms a bowl shaped region within which the CO₂ is able to sit and interact with the conjugated functionality surrounding it. Adding a further fragment of the respective polymer results in a high energy-binding site surrounded by an additional bowl shaped region and the CO₂ is therefore able to interact with further conjugated functionality. This leads to an increased binding energy of 34.14 and 35.44 kJ mol⁻¹ for P5 and P6 respectively. A further fragment of the respective polymer is added to the

existing binding site leading to binding energies of 45.86 and 42.97 kJ mol⁻¹ (SI, section 16, Tables S5 to S10). In conclusion, as the concentration of CN and associated C=C functionality increases so does the number of available high energy binding sites. This is in excellent agreement with the trend in isosteric heat of adsorption obtained experimentally for P1 through to P6.

Assessment of the high energy binding sites with three polymer fragments reveals that the N atoms of the CN functionality are located between 3 and 9 Å apart with most being at approximately 7.5 Å distance apart.

To assess the distribution of nitrile groups within the generated networks we performed a radial distribution analysis on the nitrogen atoms of the nitrile groups. Figure 6a shows the comparison of this distribution in the different polymer systems. All polymers show a peak at N-N distance of 3-5 Å reflecting the nitrogen-nitrogen distance of the nitrile groups within the respective C2 and C3 repeating units. Another peak at 8.5 Å is common to all the polymers representing the N-N distance between nearest neighbor C2 or C3 groups. P2 has the sharp peaks in the radial distribution reflecting the relatively rigid nature of the network resulting in well-defined distances between neighboring nitrile groups. The peaks become progressively broader going from P3 to P6 reflecting the range of distances available due to the flexibility of the network. For P4, P5, and P6, the peak is shifted to lower values with P5 having an additional peak at 7.8 Å (SI, section 17). This reflects the increasing concentration of CN functionality and the formation of additional high-energy CO₂ binding sites as described above.

3.4. Carbon dioxide binding

CO₂ can occupy a number of different sites within the pore structure and may be able to interact with multiple nitrile groups. To sample the sorption sites and their respective proximity to network nitrile groups we seed 10 CO₂ molecules within each network, we then perform molecular dynamics simulations and optimization sampling the radial distribution

function of the central carbon atom of the CO₂ molecules to the nitrogen atom of the network nitrile groups. The resulting radial distribution plots are shown in SI, section 18.

The plots show that the CO₂ molecule for all systems is able to sample sites with a distance of 3.5 Å to the nitrile group (Figure 6b), the distance expected for the higher binding energy sites. For P3, P4, P5, and P6 the CO₂ molecule is able to sample sites with a distance of 3.1 Å distance to a nitrile group. Furthermore, the number of times that sites of distance of 5 Å or less to a nitrile site, is greatly increased compared to P2.

To further assess the diffusion of CO₂, we perform molecular dynamic simulation of the diffusion of a molecule of CO₂ diffusing through P6. We describe the P6 polymer as fully flexible with all bonds and angles being described fully meaning that the P6 polymer is able to be flexible and dynamic. As a comparison we also perform the same diffusion experiment with P2 (Figure 6 c and d).

The CO₂ molecule is able to freely diffuse through P2 as the pore structure is large and connected. The diffusion of the CO₂ molecule is more restricted in P6 but the molecule is still able to diffuse through a large volume and sample multiple binding sites. The diffusion coefficients were calculated for each polymer. In P2, diffusion coefficients of 5.2 and 12.15 nm² ns⁻¹ were calculated reflecting diffusion in a small pore and larger pore regions of the model respectively (SI, Figure S32). In P6, a diffusion coefficient of 3.08 nm² ns⁻¹ was calculated (SI, Figure S33). The diffusion of the CO₂ in P6 is slower as the system has only small pore regions with pore diameters less than 10 Å. Closer inspection of the CO₂ diffusion trajectory in P6 shows that the molecule pathway is through pores that are surrounded by the conjugated functionality and we would hence expect that these pathways will have high energy binding sites.

3. Conclusion

In conclusion, we have successfully tuned the sorption enthalpies of carbon dioxide in amorphous polymer networks for tailor-made values by controlling the weight percentage of

cyanovinylene content. Accordingly, we designed and synthesized microporous polymers under different polymerization methods with engineered percentages of functional groups as interesting materials for carbon capture. While the networks achieved CO₂ uptakes higher than 100 mg g⁻¹, an unprecedented structure – thermodynamic-property relationship was revealed as the isosteric heats of adsorption proved to be linearly proportional to the content of the cyanovinyl group. In consequence, enthalpies were adjusted to tailor-made values by designing new polymers with the required amount of cyanovinyl bridges. An environmentally friendly metal-free condensation reaction from cheap starting materials, and only water as by-product, generated porous polymers with CO₂ sorption enthalpies as high as 40 kJ mol⁻¹, amongst the highest reported to date for physisorption in MPNs and exhibiting exceptional selectivities close to 100. TPD measurements and VSA technique confirmed the physical nature of the sorption while regeneration of the polymer was achieved at slight under-pressure and ambient temperature, or at 80°C and under normal pressure. Thorough theoretical calculations and dynamic simulations of the amorphous polymers showed that the binding sites form a bowl shaped region for CO₂ adsorption and that these sites increase with the concentration of CN and associated C=C functionality in the networks.

Although these materials are not meant to be directly used for commercial application, the explored structure-property relationships in this study could draw the attention for new design rules of future polymers with advanced CO₂ capture properties. Moreover, their precisely controlled structures might give them high advantages as additives in mixed membranes for gas separation applications,^[26] the issue we are currently developing with our materials.

4. Experimental Section

Experimental details including crystallography data, full synthetic procedures, FT-IR, Elemental Analysis and NMR spectra, PXRD measurements, gas sorption properties, theoretical calculations and dynamic simulations are available in Supporting Information.

CCDC 1440645 contains the supplementary crystallographic data for this paper. These data can be obtained free of charge from The Cambridge Crystallographic Data Centre via www.ccdc.cam.ac.uk/data_request/cif

Supporting Information

Supporting Information is available from the Wiley Online Library or from the corresponding authors.

Acknowledgements

A.Y. acknowledges funding from the European Research Council within the project 278593_ORGZEO. We thank Elisabeth Irran for single-crystal Xray diffraction and Anton Sagaltchik of BasCat, the joint UniCat-BASF lab at TU Berlin, for assistance in TPD.

Received: ((will be filled in by the editorial staff))

Revised: ((will be filled in by the editorial staff))

Published online: ((will be filled in by the editorial staff))

- [1] IEA. World energy outlook, **2015**; BP. BP energy outlook 2035. January **2014**. Tech. rep. 2014.
- [2] S.H. Mohr, J. Wang, G. Ellem, J. Ward and D. Giurco, *Fuel*, **2015**, 141, 120.
- [3] Fourth Assessment Report of the Intergovernmental Panel on Climate Change, **2007**. Summary for Policymakers.
- [4] S. Suranovic, *Global Environmental Change*, **2013**, 23, 598.
- [5] M. Kanniche, R. Gros-Bonnivard, P. Jaud, J. Valle-Marcos, J.-M. Amann, C. Bouallou, *Applied Thermal Engineering* **2010**, 30, 53.
- [6] C.-H. Yu, C.-H. Huang, C.-S. Tan, *Aerosol and Air Quality Research*, **2012**, 12, 745.
- [7] A.H. Lu, G.P. Hao, *Annu. Rep. Prog. Chem., Sect. A: Inorg. Chem.* **2013**, 109, 484.
- [8] a) A. Thomas. *Angew. Chem. Int. Ed.* **2010**, 49, 8328; b) A.I. Cooper, *Adv. Mater.* **2009**, 21, 1291; c) Y. Xu, S. Jin, H. Xu, A. Nagai, D. Jiang, *Chem. Soc. Rev.* **2013**, 42, 8012.

- [9] R. Dawson, E. Stockel, J.R. Holst, D.J. Adams, A.I. Cooper, *Energy Environ. Sci.*, **2011**, 4, 4239.
- [10] R. Dawson, L. Stevens, T. Drage, C. Snape, M. Smith, D.J. Adams, A.I. Cooper, *J. Am. Chem. Soc.* **2012**, 134, 10741.
- [11] R. Dawson, D.J. Adams, A.I. Cooper, *Chem. Sci.*, **2011**, 2, 1173.
- [12] a) W. Lu, J. Sculley, D. Yuan, R. Krishna, Z. Wei, H.C. Zhou, *Angew. Chem. Int. Ed.* **2012**, 51, 7480; b) W. Lu, W. Verdegaal, j. Yu, P. Balbuena, H.K. Jeong, H.C. Zhou, *Energy Environ. Sci.* **2013**, 6, 3559.
- [13] a) H. Patel, F. Karadas, J. Byun, J. Park, E. Deniz, A. Canlier, Y. Jung, M. Atilhan, C.T. Yavuz, *Adv. Funct. Mater.* **2013**, 23, 2270; b) D. Ko, H. Patela, C.T. Yavuz, *Chem. Commun.* **2015**, 51, 2915.
- [14] R. Dawson, A.I. Cooper, D.J. Adams, *Polym. Int.* **2013**, 62, 345.
- [15] K. Sumida, D. Rogow, J.A. Mason, T.M. McDonald, E.D. Bloch, Z.R. Herm, T.H. Bae, J.R. Long, *Chem. Rev.* **2012**, 112, 724.
- [16] A. Torrisi, R.G. Bell, C. Mellot-Draznieks, *Cryst. Growth Des.* **2010**, 10, 2839.
- [17] Q. Bricaud, A. Cravino, P. Leriche, J. Roncali, *Synt Met.* **2009**, 159, 2534.
- [18] a) J. Schmidt, M. Werner, A. Thomas, *Macromolecules* **2009**, 42, 4426; b) W. Lu, D. Yuan, J. Sculley, D. Zhao, R. Krishna, H.C. Zhou, *J. Am. Chem. Soc.*, **2011**, 133, 18126.
- [19] M. Trunk, A. Herrmann, H. Bildirir, A. Yassin, J. Schmidt, A. Thomas, *Chem. Eur. J.* **2016**, 22, 7179.
- [20] A. Uptmoor, J. Freudenberg, T. Schwäbel, F. Paulus, F. Rominger, F. Hinkel, U. Bunz, *Angew. Chem. Int. Ed.* **2015**, 54, 14673.
- [21] A.L. Myers, J.M. Prausnitz, *AIChE Journal* **1965**, 11, 121.
- [22] Y. Lim, I. Choi, H. Lee, I.W. Kim, J.Y. Chang, *J. Mater. Chem. C*, **2014**, 2, 5963.
- [23] a) A. Yassin, P. Leriche, J. Roncali, *Macromol. Rapid Commun.*, **2010**, 31, 1467; b) A. Yassin, R. Mallet, P. Leriche, J. Roncali, *ChemElectroChem* **2014**, 1, 1219.

[24] Y. Zhao, X. Liu, Y. Han, *RSC Adv.*, **2015**, *5*, 30310.

[25] A. Kumar, D.G. Madden, M. Lusi, K.J. Chen, E. Daniels, T. Curtin, J. Perry, M. Zaworotko, *Angew. Chem. Int. Ed.* **2015**, *54*, 14372.

[26] C. Xu, N. Hedin, *Mater. Today*, **2014**, *17*, 397.

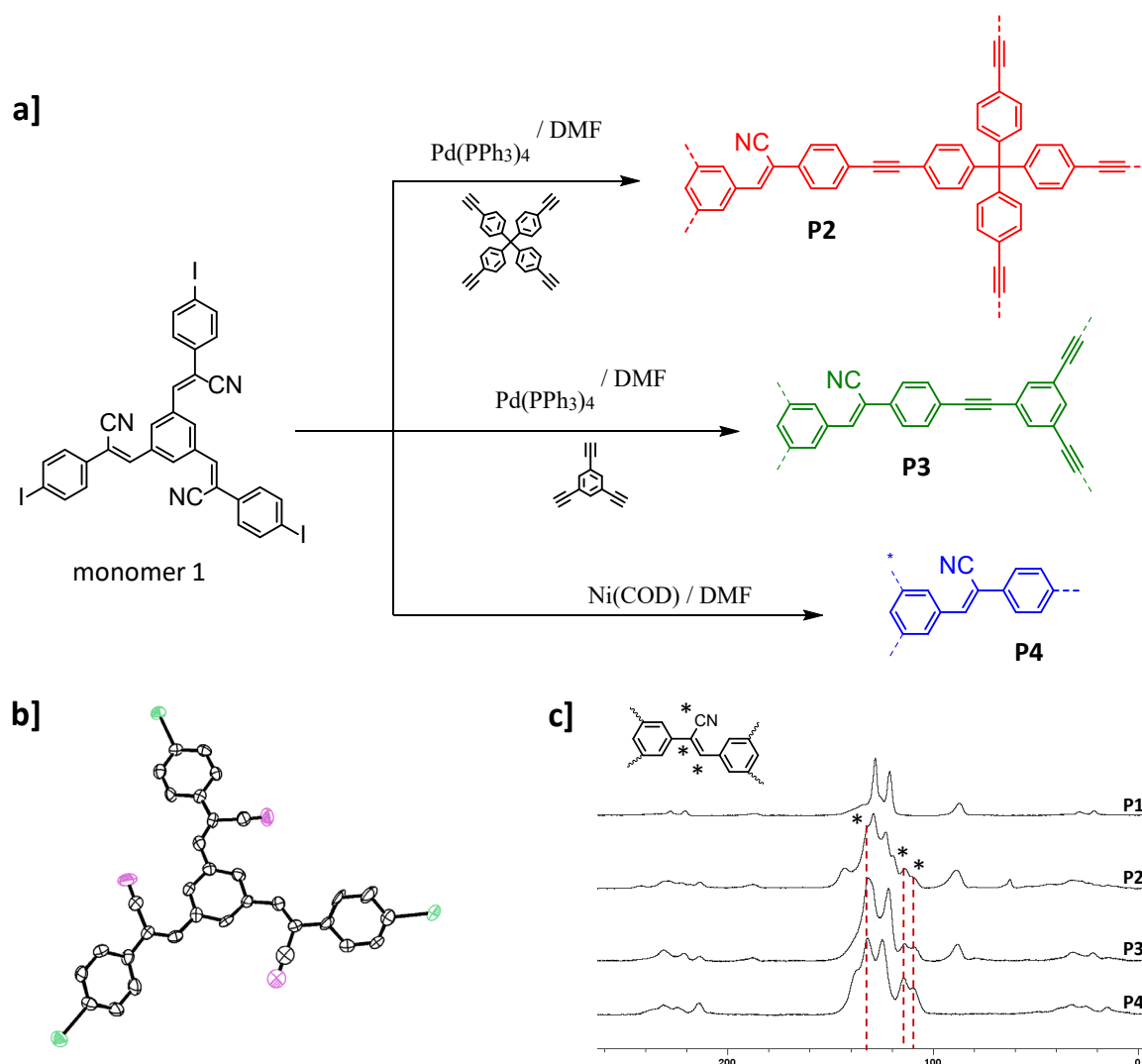


Figure 1. a) Metal-catalyzed reactions of monomer 1 under different conditions for MPNs **P2**, **P3** and **P4**, b) Single crystal X-ray resolved structure of the monomer, c) ^{13}C solid state NMR of the MPNs showing the chemical shifts corresponding to the cyanovinyl moiety, and their absence in **P1**.

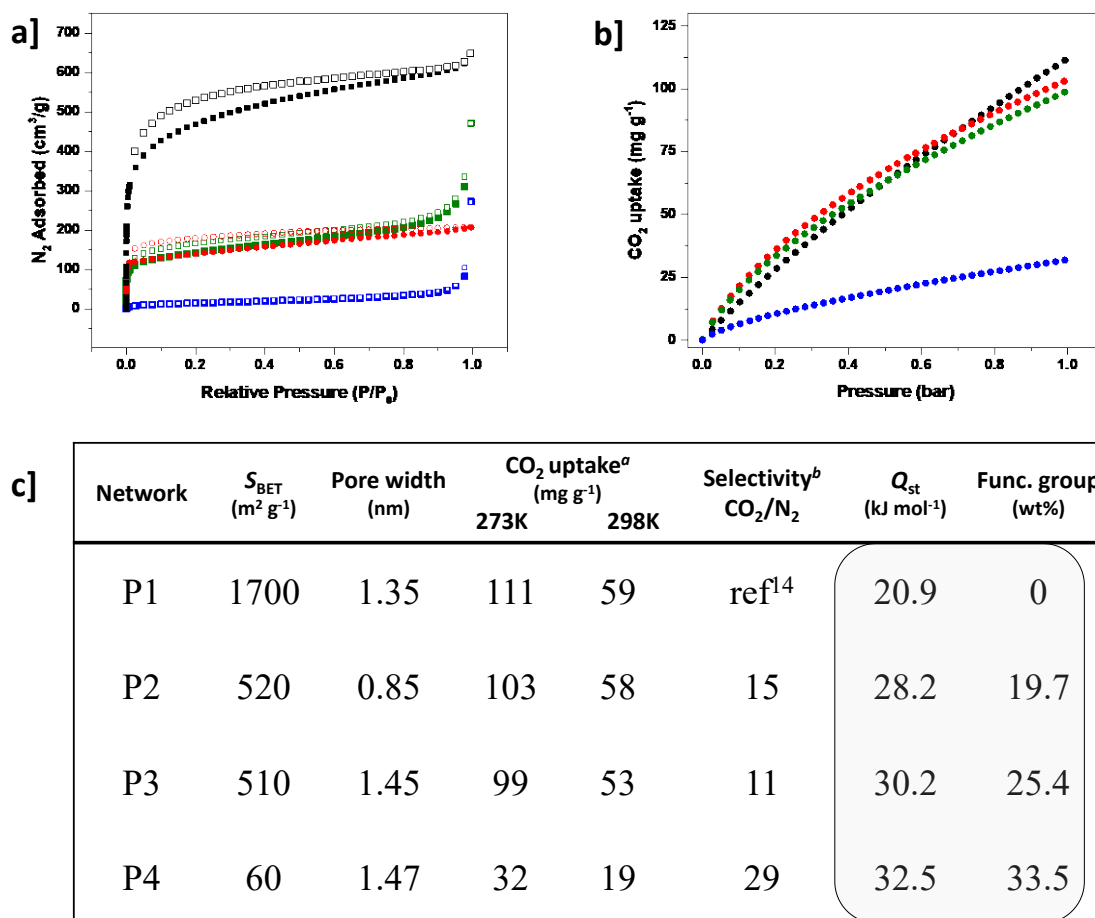
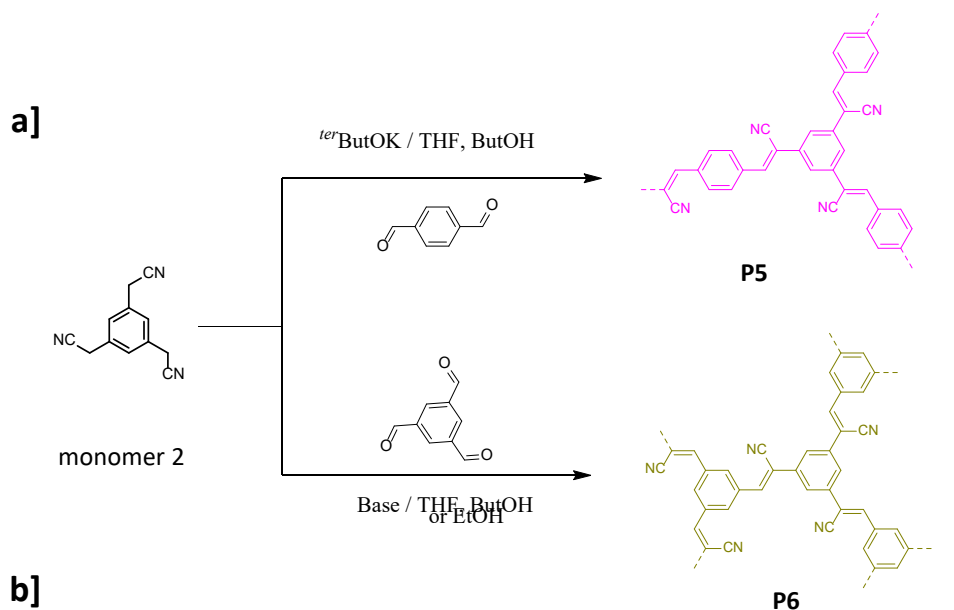


Figure 2. a) N_2 adsorption (solid) and desorption (hollow) isotherms of the metal-catalyzed networks at 77 K; b) CO_2 uptakes at 273 K. **P1** (black), **P2** (red), **P3** (green) and **P4** blue, c) Gas sorption properties of the metal-catalyzed polymers. ^auptakes at 1 bar. ^bSelectivities at flue gas conditions (85:15 / $\text{N}_2:\text{CO}_2$). Wt% represents the percentage of $\text{C}_3\text{H}_1\text{N}$ per repeating unit of polymer (see S2).



b]

Network	S_{BET} ($\text{m}^2 \text{g}^{-1}$)	CO_2 uptake (mg g^{-1})	Selectivity CO_2/N_2	Q_{st} (kJ mol^{-1})	Func. group (wt%)
P5	80	59	74	38.5	44.7
P6	112	90	96	40.3	50.5

c]

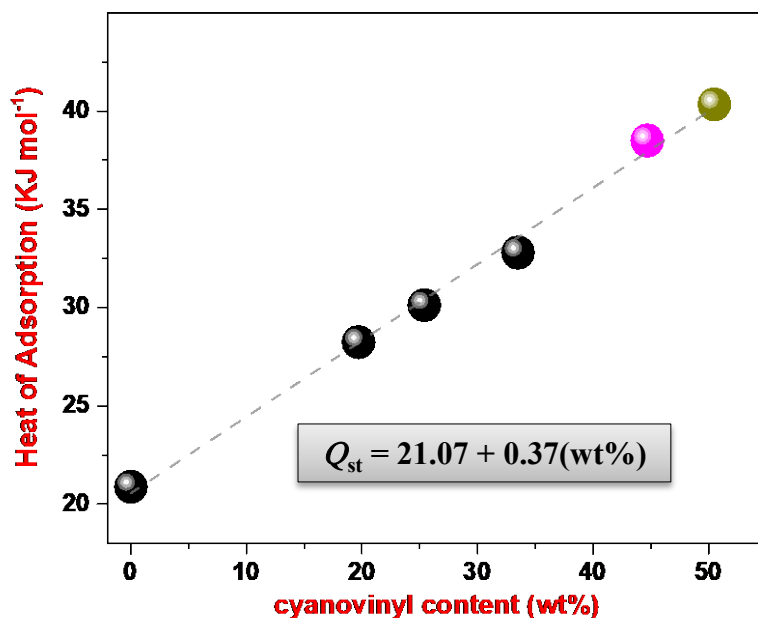


Figure 3. a] Metal-free condensation under basic conditions for **P5** (pink) and **P6** (dark yellow), b] Gas sorption properties of the two polymer networks. c] The linear relationship between Q_{st} and the wt% of cyanovinyl content in the networks. The best fitting line is dashed. **P5** (pink) and **P6** (dark yellow).

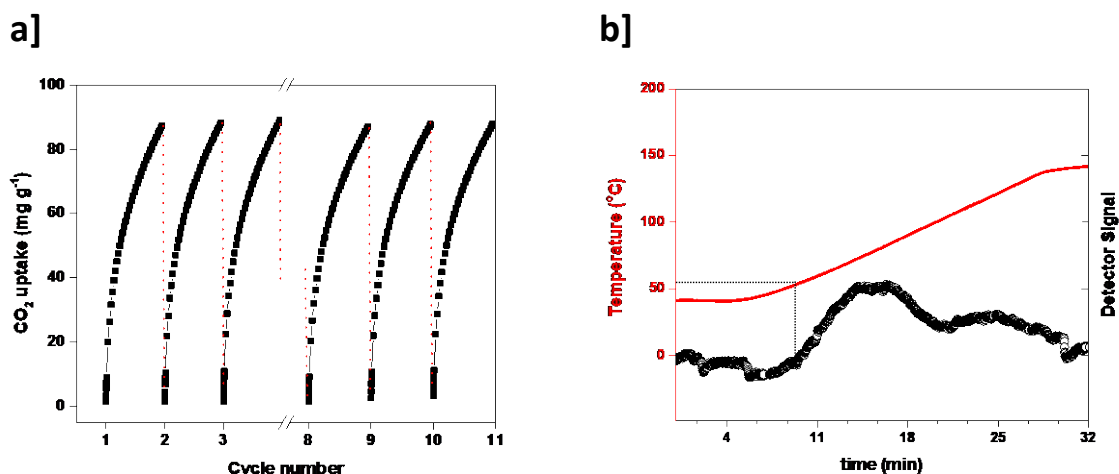


Figure 4. a) CO₂ isotherms for **P6** at 273 K and 1 bar, the material being cycled 10 times. Each regeneration step takes an average of 4 min at 1 mbar, b) TPD plot for **P6**. In red is denoted the temperature ramp profile used for desorption. The signal for CO₂ is given by the black curve

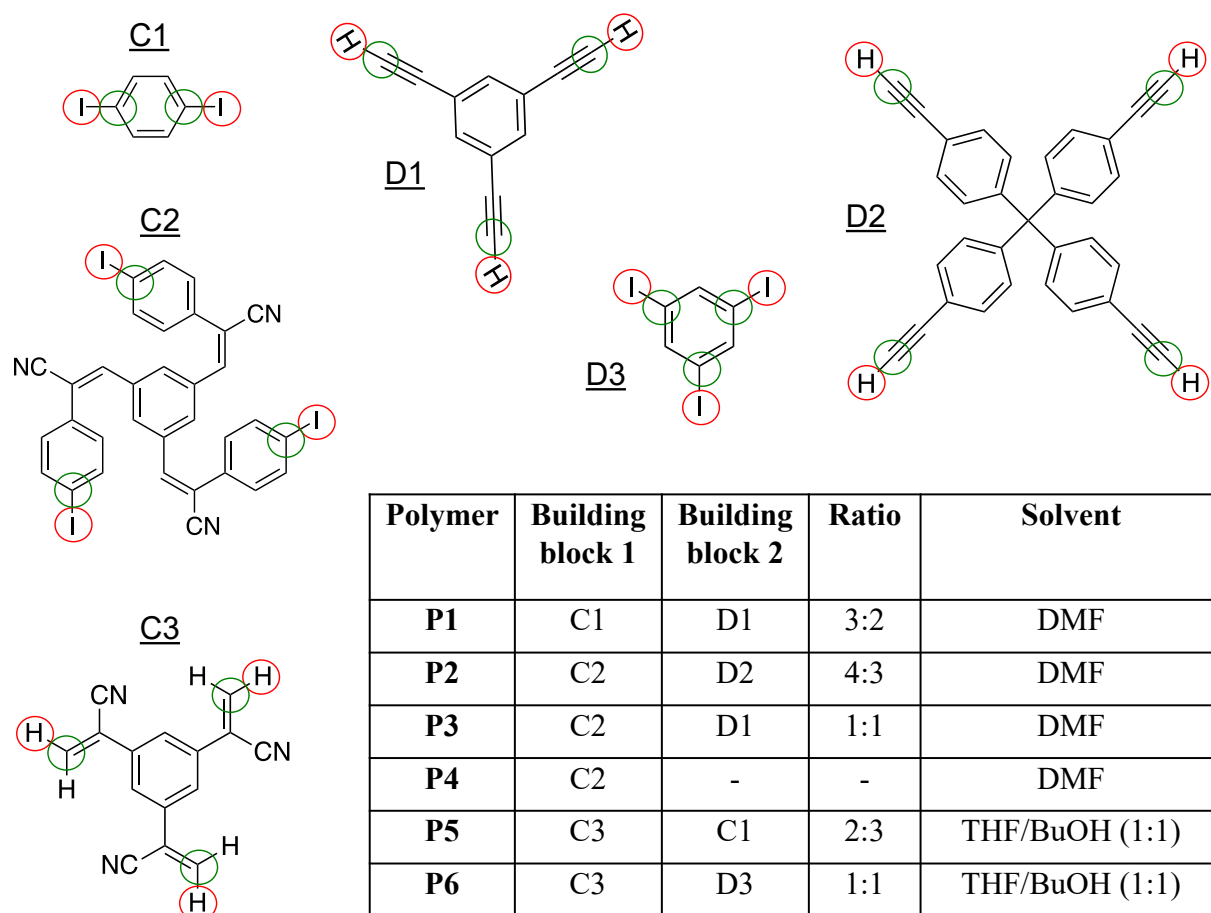


Figure 5. Structures optimized using DFT as building blocks for the construction of the network models. Atoms with a red circle are the designated cap atoms, and with a green circle are the end groups. Once a bond is formed the cap atoms are removed. The table shows the building block ratios for the respective polymer model systems.

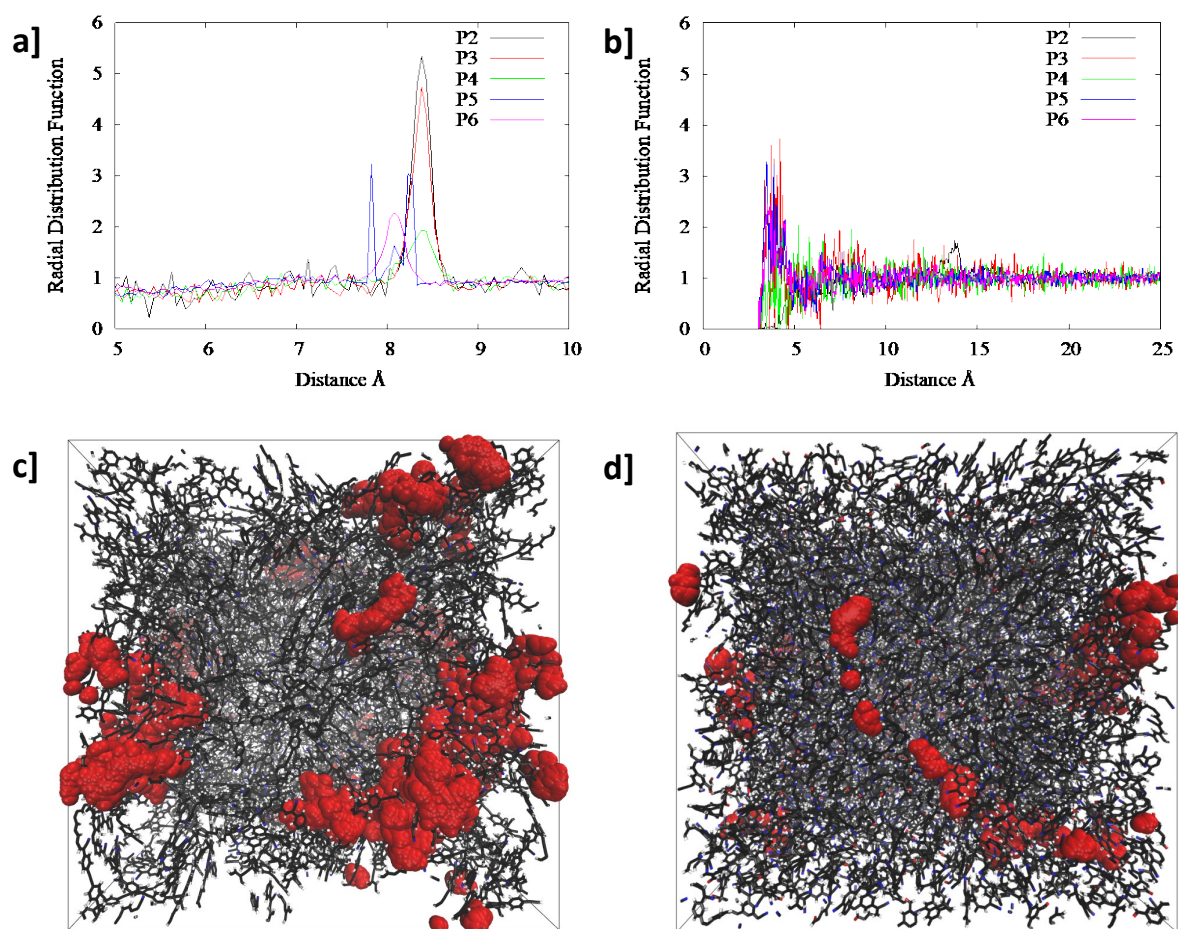


Figure 6. a) Comparison of the radial distribution of N in the polymers, b) and comparison of the radial distribution of the C atom, in CO₂, to the N of the polymers, c) Overlay of CO₂ diffusion in P2, and d) CO₂ diffusion in P6

The table of contents entry should be 50–60 words long, and the first phrase should be bold. The entry should be written in the present tense and impersonal style. The text should be different from the abstract text.

Carbon capture • Cyanovinylene microporous polymers • Structure – property relationships • Amorphous polymers modeling • Sorption enthalpy

A. Yassin,* M. Trunk, F. Czerny, P. Fayon, A. Trewin, J. Schmidt, A. Thomas*

Structure – Thermodynamic-property Relationships in Cyanovinyl-based Microporous Polymer Networks for the Future Design of Advanced Carbon Capture Materials

ToC figure ((Please choose one size: 55 mm broad × 50 mm high or 110 mm broad × 20 mm high. Please do not use any other dimensions))